Formation and evolution of the C-type asteroid 162173 Ryugu: Evidence from returned samples analyzed by X-ray micro- and nano-tomographies

1. Introduction

The samples collected from the surface of the C-type asteroid 162173 Ryugu were successfully brought back to Earth on 6th December 2020 by the Hayabusa2 spacecraft of Japan Aerospace Exploration Agency (JAXA) [1]. The initial analytical campaign was performed for one year from June 2021 after noninvasive and nondestructive curatorial works at JAXA. Further detailed analyses by JAXA "International Announcement of Opportunity (AO) for Hayabusa2 Sample Investigation" are under way. Our research group performed a series of multiscale nondestructive three-dimensional (3D) analyses by combining different types of X-ray tomography (XCT) as the initial analysis [2,3] and advanced curatorial work [4]. Through these analyses, we revealed the features of the returned samples and their relation to known meteorites. We also performed further analyses to understand the origin and evolution of Ryugu and the evolution processes on the asteroid surface. The results were also useful for cutting cross sections appropriate for later analyses such as electron microscopy.

The returned samples are composed of particles of $<\sim 10$ mm size [1,5] (Fig. 1). The total amount of the samples is ~ 5.42 g. To perform appropriate and systematic analyses, we used two different beamlines using different XCT imaging systems for different particle size ranges: large particles of $>\sim 100$ μm size at SPring-8 BL20XU and small particles of $<\sim 100$ μm size at SPring-8 BL47XU. In this review, we described the features of the two beamlines and the results obtained thus far separately.

2. Analysis at SPring-8 BL20XU for large samples

The integrated XCT system using 30 keV X-ray beams equipped at beamline BL20XU was used for large samples ($>\sim 100$ μm). This system is composed of three types of XCT: absorption X-ray tomography (absorption-CT), X-ray diffraction tomography (XRD-CT), and differential phase contrast tomography (phase-CT) with a common sample stage that can be used by moving the optical devices of the three CT types [2,4], enabling us to compare their CT images easily. In the absorption-CT mode, we obtained 3D-CT images of high spatial resolution ($>\sim 0.85$ μm/voxel) in a wide field of view ($<\sim 3$ mm) by using a 4K camera. In the XRD-CT mode, mineral phases were identified from the obtained XRD pattern and 2D mineral maps were constructed in arbitrary cross sections. In the phase-CT mode, low-element materials with low absorption, such as carbonaceous materials, were observed. Through these modes, we performed not only textural observation but also the identification of constituent mineral phases.

Extraterrestrial samples such as Ryugu samples might undergo alterations such as oxidation and hydration through contact with the terrestrial atmosphere. Each Ryugu sample, which was set in a container filled with dry and pure N_2 gas, was transferred from the JAXA curation facility. To exclude atmospheric exposure, we prepared a special glove box filled with dry and pure N_2 gas. The sample was moved to a sample holder for CT and the holder was sealed (Fig. 2) in the glove box [6].

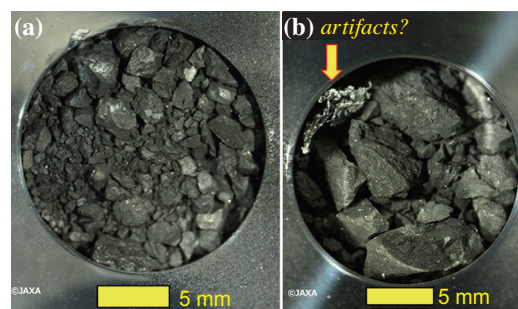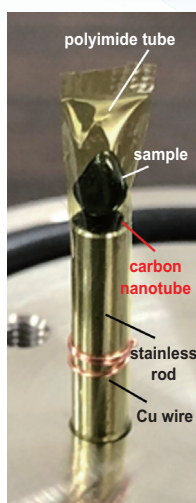We examined 24 Ryugu particles (1.8–8.7 mm in size or 0.8–93.5 mg

Fig. 1. All samples returned from the asteroid Ryugu (courtesy of JAXA). Samples in Chambers A **(a)** and C **(b)** were collected during the first and second touch-down operations (TD1 and TD2), respectively [5]. TD2 was performed near the artificial crater excavated using the small carry-on impactor (SCI) [1].

Fig. 2. Sample holder for CT at BL20XU. A sample particle placed on a carbon nanotube sheet is sealed with a polyimide tube and a Cu wire. The polyimide tube is filled with dry and pure N_2 gas.

in weight) [2,4]. The optical and absorption-CT slice images of a typical sample particle are shown in Figs. 3(a,b). The contrast of the CT image corresponds to the linear absorption coefficient of the material, which is determined by the chemical composition and density. In Ryugu samples, regions with bright and dark contrasts generally correspond to Fe-rich and Fe-poor materials, respectively. However, Ca-rich phases also show some bright contrasts, and porous regions have dark contrasts. Therefore, we used XRD-CT to confirm their mineral phases. As shown in Fig. 3(b), Ryugu samples are generally composed of mineral grains of pyrrhotite ($Fe_{1-x}S$), magnetite (Fe_3O_4), dolomite ($CaMg(CO_3)_2$), and breunnerite (($Mg,Fe)CO_3$) embedded in a fine matrix of phyllosilicates (saponite: $(Ca/2,Na)_{0.3}$ $(Mg,Fe)_3((Si,Al)_4O_{10}(OH)_2 \cdot nH_2O$ and serpentine: $(Mg,Fe)_3Si_2O_5(OH)_4$). The mineral assemblage and its texture clearly showed that Ryugu samples correspond to Ivuna-type carbonaceous chondrites (CI) (e.g., [7]) or related material [2,4]. We observed heterogenous contrasts with a spatial scale of 1 mm or less in the matrix (Fig. 3(b)). On the

basis of these results, the samples were prepared using a wire saw to obtain designated areas for later destructive analyses, and then many scientific outcomes were obtained efficiently [2,4].

The volumes of the sample particles were obtained from the absorption-CT images. The bulk densities of 16 particles were determined together with their masses separately measured using a precise electric balance. It is difficult to measure the volume of relatively small and fragile samples such as Ryugu particles. However, the present method of using XCT would be most reliable. The value ranges from 1.65 to 1.93 g/cm^3 with an average of 1.79±0.08 g/cm^3 [2]. The bulk density of large CI chondrite grains varies from 1.58 to 1.91 g/cm^3, which should be the result of alteration on Earth (terrestrial weathering). The bulk density of Ryugu particles determined in the present study is one of the most important physical properties and the present value was used to discuss dynamical processes, such as the formation and impact fragmentation of Ryugu, and physicochemical processes, such as aqueous alteration in Ryugu [2].

Cracks were observed in most of the samples (e.g., Fig. 3(b)). Some flat particles have many cracks almost parallel to the flat surfaces (Figs. 3(c,d)), as a compressive deformation caused by the impact

of asteroids on Ryugu's parent body. The rubble pile asteroid of Ryugu was formed by the accumulation of such impact-induced fragments. These samples are fossils of the impact responsible for Ryugu formation [2,8].

3. Analysis at SPring-8 BL47XU for small samples

We used an analytical X-ray nanotomography (XnCT) system for small particles ($<\sim100$ μm) in BL47XU, where dual-energy tomography (DET) and scanning-imaging X-ray microscopy (SIXM) were combined (e.g., [9]). In DET, we used an imaging-absorption CT system with a voxel size of ~50 nm. Samples were imaged at two different X-ray energies (7 and 7.35 keV) near the K-edge energy of Fe (7.11 keV), enabling us to discriminate many minerals because the images at 7 and 7.35 keV roughly correspond to the z (average atomic number) and Fe contrasts, respectively. We also obtained enlarged images for ROI in 17 samples with higher resolution (~10 nm/voxel) using a common sample stage for local CT. In SIXM, we obtained differential phase shift images corresponding to density-contrast images at 8 keV with a voxel size of ~100 nm. These images are suitable for observing low-element materials, such as water and organic materials. By combining these sets of CT images, we obtained 3-color CT images (R: absorption image
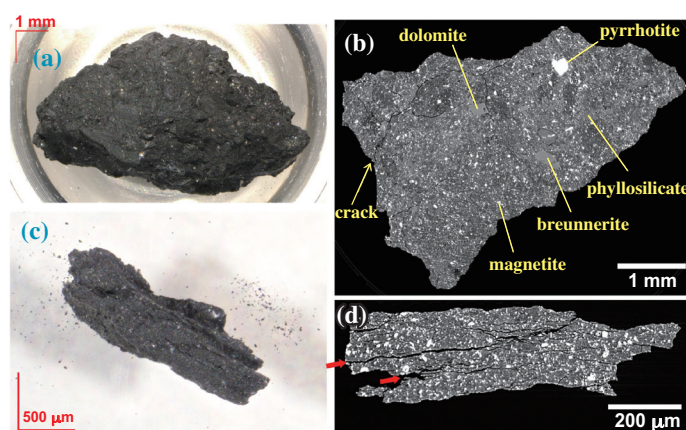
Fig. 3. Optical and absorption CT images of large Ryugu particles. (a,b) Sample: C0002. (c,d) Sample: C0055.
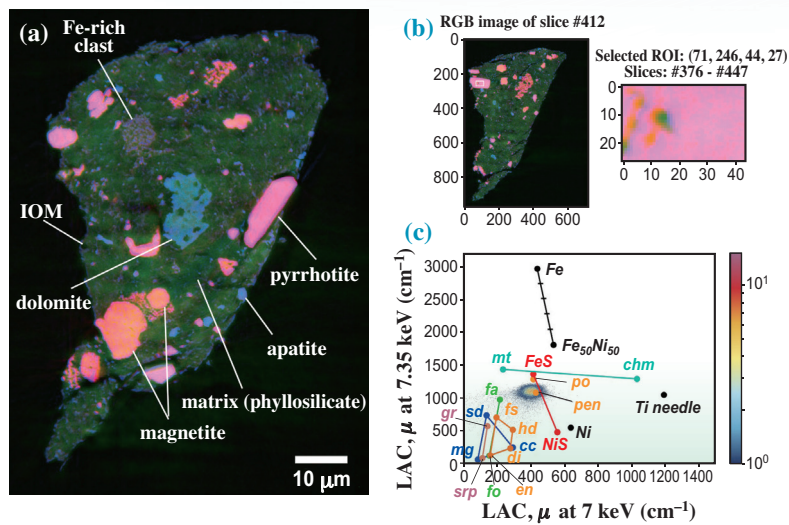
Fig. 4. 3-color CT images of small Ryugu particles (sample: C0103-FC007) and method of quantitative mineral discrimination. **(a)** 3-color CT image of R (LAC at 7 keV = 0-950 cm⁻¹), G (RID = 0-20×10⁻⁶), and B (LAC at 7.35 keV = 0-450 cm⁻¹). **(b)** ROI for pink mineral used for the mineral discrimination. **(c)** 2D histogram of LAC at 7 keV *vs* LAC at 7.35 keV for ROI in (b), indicating the pink mineral is pyrrhotite. The other 2D histograms of LAC at 7 keV *vs* RID and LAC at 7.35 keV *vs* RID were also considered but are not shown here. LAC: linear attenuation coefficient. RID: refractive index decrement (= 1 − refractive index ∝ ~density). *mt*: magnetite, *chm*: chromite, *po*: pyrrhotite, *pen*: pentlandite, *fa*: fayalite, *fo*: forsterite, *fs*: ferrosilite, *hd*: hedenbergite, *di*: diopside, *en*: enstatite, *gr*: greenalite, *srp*: serpentine, *sd*: siderite, *cc*: calcite, and *mg*: magnesite.

at 7.35 keV, G: phase image, and B: absorption image at 7 keV), and the distributions of different minerals, organic materials, pores, and cracks are easily recognized in 3D (Fig. 4(a)). Quantitative phase discrimination was based on the contrast histograms of the three sets of CT images (Figs. 4(b,c)).

We examined 54 samples (9–103 μm in sphere-equivalent diameter) [2,4,10]. Most of them were small particles recovered, and some were extracted from large particles. The 3-color CT slice image of a typical sample is shown in Fig. 4(a). Different mineral grains (pyrrhotite, magnetite, dolomite, and apatite: $Ca_5(PO_4)_3(F,Cl,OH)$) were embedded in a fine-grained matrix of phyllosilicates. Organic materials (insoluble organic matter: IOM) and voids were also seen. The mineral assemblages and textures are also consistent with those of CI chondrites and related materials. We, however, have not completed the observation of some minerals such as sulphates in

CI, and this can be explained by the terrestrial weathering of CI.

Pyrrhotite and carbonate (dolomite and breunnerite) grains, which precipitated from aqueous fluid during aqueous alteration in Ryugu is parent body, contained a large number of

pores in CT images, some of which would be occupied by low-density materials (Figs. 5(a,b)). A relatively large inclusion (~3 μm) in pyrrhotite (Fig. 5(a)) was exposed by an ion beam at –120°C below the freezing temperature of the fluid and analyzed by time-of-flight secondary ion mass spectroscopy (TOF-SIMS). Ion signals from H_2O and CO_2 indicated that this inclusion was filled with H_2O–CO_2 fluid (or liquid) (Fig. 5(c)) [2]. Aqueous fluid has been found in a carbonaceous chondrite [11], but this is the first discovery of aqueous fluid in a known asteroid. The presence of CO_2 strongly suggests that Ryugu's parent body was formed outside of the CO_2 snow line in the outer region of the Solar System beyond the Jupiter orbit and transferred to the asteroid belts between Mars and Jupiter. The TOF-SIMS signals also indicate that the fluid is brine like ocean water. IOM was observed in pyrrhotite and carbonates (Fig. 5(b)), suggesting that IOM particles were dispersed in an aqueous fluid.

Crystal morphologies of minerals in 3D were examined. Magnetites have a large variety of morphologies (e.g., spherulite, framboid (Fig. 6(a)), plaquette, bar, and equant), while
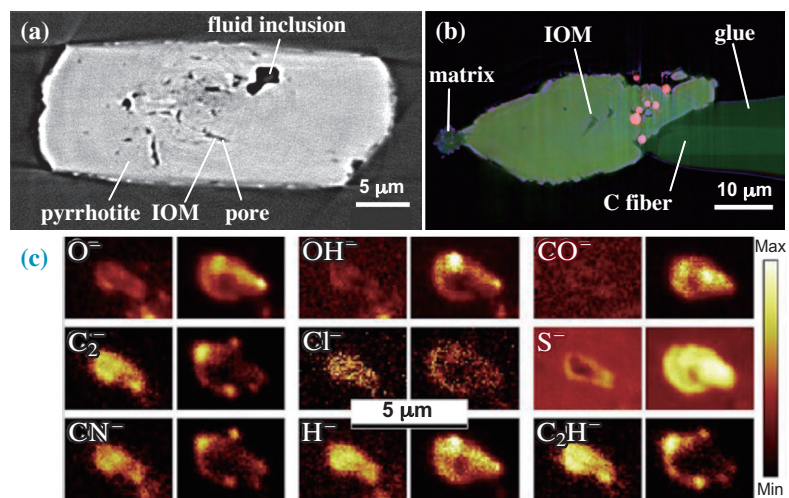
Fig. 5. Fluid and IOM inclusions. **(a)** Absorption CT image (7 keV) of pyrrhotite grain containing fluid and IOM inclusions (sample: C0002-FC012). **(b)** 3-color CT image of breunnerite grain containing IOM inclusions (LAC and RID ranges are the same as those in Fig. 4(a) (sample: A0067-FC0003). **(c)** TOF-SIMS ion maps of fluid inclusion in (a) [2].
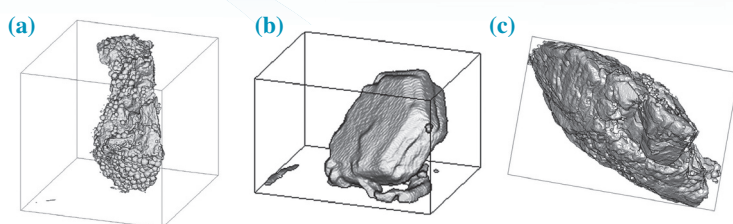
Fig. 6. Bird's-eye views of mineral grains created from 3D absorption CT images. **(a)** Framboidal magnetite crystals covering on a sample particle surface, ~45 μm in length (sample: A0104-00000900). **(b)** Hexagonal plate grain of pyrrhotite, $8 \times 5.5 \times 2.5$ μm in size (sample: A0104-00000900). **(c)** Flat rhombohedral grain of breunnerite, $49 \times 42.5 \times 17$ μm in size (sample: A0067-FC003).

other minerals have rather simple morphologies with facets (pyrrhotite: hexagonal plate (Fig. 6(b)), dolomite and breunnerite: flat rhombohedron (Fig. 6(c)), and apatite: hexagonal prism). From the included and enclosed relations among these minerals in 3D, their order of precipitation was estimated. On the basis of the obtained results, we proposed a model for the formation and evolution of Ryugu's parent body: formation by the accumulation of CO_2–H_2O ice, minerals (mainly amorphous silicate and Fe sulfide), and IOM, and the subsequent aqueous alteration by the reaction of the minerals with melted ice, where magnetite with irregular morphologies (e.g., spherulite, framboid, and plaquette) and poorly crystalline phyllosilicates precipitated first from a highly supersaturated aqueous fluid formed by the rapid dissolution of amorphous silicates, followed by the precipitation minerals with simple morphologies and coarse phyllosilicates from a slightly supersaturated aqueous fluid [10].

We also observed amorphization in a "smooth layer" [3], melts (glasses) (Fig. 7) in a "frothy layer" [3], and craters on the surfaces of Ryugu particles [2,3]. They are the results of space weathering caused by the exposure of solar wind and micrometeoroid bombardments. The absorption of the 2.7 μm hydroxyl (–OH) band in the reflectance IR spectrum of the Ryugu sample was determined to be stronger than that

of the Ryugu surface determined by Hayabusa2 remote sensing observation [2]. This discrepancy can be explained by the dehydration of the outermost surface of space-weathered grains on the Ryugu surface, which contributes to the weakening of the 2.7 μm band [3].

4. Summary

We performed the 3D analysis of returned samples from the asteroid Ryugu by combining different types of XCT systems at SPring-8 BL20XU and BL47XU for 24 large (>~100 μm) and 54 small (<~100 μm) particles, respectively. We revealed that the returned samples correspond to CI chondrites or related materials [2,4,5]. This is consistent with the results of other mineralogical, petrological, and geochemical analyses (e.g., [2,4,12]). CI chondrites are one of the most important meteorites
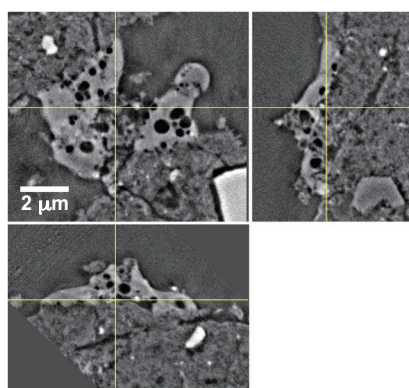
Fig. 7. Absorption CT image (7.35 keV) of melt splash (vesiculated glass) on particle surface (sample: C0105-04300900).

because they exhibit a representative chemical composition of the Solar System (e.g., [7]). We revealed physical, mineralogical, and petrological characteristics of these important Ryugu samples, such as bulk density, impact features, space weathering, crystal morphology, and mineral precipitation order during aqueous alteration. We discovered CO_2–H_2O fluid, suggesting the formation of Ryugu's parent body in the outer region of the Solar System. Detailed analyses by AO are now still under way.

Akira Tsuchiyama[a,b,c,*]
and Megumi Matsumoto[d]

[a] Research Organization of Science and Technology, Ritsumeikan University
[b] CAS Key Laboratory of Mineralogy and Metallogeny/Guangdong Provincial Key Laboratory of Mineral Physics and Materials, Guangzhou Institute of Geochemistry, China
[c] CAS Center for Excellence in Deep Earth Science, China
[d] Department of Earth and Planetary Materials Sciences, Tohoku University

*Email: atsuchi@fc.ritsumei.ac.jp

References

[1] S. Tachibana et al.: Science **375** (2022) 1011.
[2] T. Nakamura et al.: Science **379** (2023) 787.
[3] T. Noguchi et al.: Nat. Astron. **7** (2023) 170.
[4] M. Ito et al.: Nat. Astron. **6** (2022) 1163.
[5] T. Yada et al.: Nat. Astron. **6** (2022) 214.
[6] M. Uesugi et al.: Rev. Sci. Instrum. **91** (2020) 035107.
[7] D. S. Lauretta and H. Y. McSween Jr.: Eds. "Meteorites and the Early Solar System II," p.942 (2006), The University of Arizona Space Science Series.
[8] M. Kikuiri et al.: MetSoc 2022 (2022) Abstract #6199.
[9] M. Matsumoto et al.: Science Adv. **5** (2019) eaax5078.
[10] A. Tsuchiyama et al.: MetSoc 2022 (2022) Abstract #6221.
[11] A. Tsuchiyama et al.: Science Adv. **7** (2021) eabg9707.
[12] T. Yokoyama et al.: Science **379** (2023) 786.